

The Gaussian impurity effect on the electronic and magnetic properties of an electron confined in a lateral quantum dot

Ayham Shaer, Mohammad K. Elsaid

Physics Department, An-Najah National University, Nablus, Palestine

Corresponding author: Ayham Shaer, ayham.shaer@najah.edu

ABSTRACT The Hamiltonian of a single electron trapped in a lateral quantum dot in the influence of an acceptor Gaussian impurity has been solved using a variational wavefunction as a superposition of a product of eigenfunctions of the harmonic oscillator in x and y coordinates. The effects of Gaussian impurity parameters on the system's spectra have been investigated as a function of the magnetic field. Furthermore, the electron probability has been displayed to investigate the impurity position effect on the energy levels. As a second step, the calculated energy spectra were utilized to compute and visualize the system's magnetic properties in the presence of the magnetic field and impurity. The obtained energy spectra show level crossings in the presence of acceptor impurity, which causes oscillations in the magnetic susceptibility and magnetization curves, resulting in an exciting diamagnetic–paramagnetic phase transition.

KEYWORDS lateral quantum dot, magnetic properties, Gaussian impurity, diamagnetic-paramagnetic transition

FOR CITATION Shaer A., Elsaid M.K. The Gaussian impurity effect on the electronic and magnetic properties of an electron confined in a lateral quantum dot. *Nanosystems: Phys. Chem. Math.*, 2022, **13** (3), 265–273.

1. Introduction

The electrical, thermal, optical, and magnetic properties in quantum-confined systems have recently got much attention. The advancements in semiconductor technology have made it feasible to develop structures with features that are particularly sensitive to heterostructure confinement, which has piqued interest. For example, by using an external magnetic field, the electronic states of the carriers confined in the quantum dot (QD) may be significantly altered [1–15]. This important topic has been well researched. Impurities also have an important influence in modifying the characteristics of semiconductor materials [13–16]. Since the ionized impurities comprise an extra attractive or repulsive electrostatic potential in the quantum dot's Hamiltonian, doping the quantum dot with acceptor and donor impurities alters the quantum confinement.

Various theoretical studies have been devoted to solving the Schrodinger equation for the QD system using various approaches such as the variational [13, 17, 18], the $1/N$ expansion [11, 12], and the exact diagonalization method [19–21].

The exact diagonalization method was used to study the magnetization and magnetic susceptibility of a donor impurity in a parabolic GaAs QD by Alia et al. [19]. The results of calculations have revealed that the electric field can modify the magnetic properties of the GaAs QD, causing its magnetic susceptibility to change from diamagnetic to paramagnetic.

The effect of the spin-orbit interaction (SOI) on the electron magnetic properties of a parabolic InAs QD has been investigated by Voskoboinikov et al. [22]. The work gives a theoretical investigation of the influence of SOI on the electron magnetic properties of tiny semiconductor QDs. At low temperatures, these properties exhibit quite exciting behavior. The sudden variations in magnetic properties at low magnetic fields are attributable to the alternate crossing of the spin-split electron levels in the energy spectrum, primarily caused by SOI. Hosseinpour [23] provided an investigation into the influence of Rashba SOI and Gaussian impurity on the heat capacity of an asymmetric QD. Madhav et al. [24] investigated the electronic properties of anisotropic QDs in a magnetic field. They also calculated a two-electron system's energy spectrum and pair-correlation function to examine the influence of inter-electron interaction on isotropic and anisotropic quantum dots.

The paper is organized as follows. Section II presents the Hamiltonian of a doped Gaussian impurity in an isotropic QD, the computation of energy spectra, and the magnetic properties of the QD. The numerical results and related discussions are given in section III, while the last section presents the conclusion.

2. Theory

This section contains the QD Hamiltonian under the effect of Gaussian impurity, the variational procedure, and the QD magnetic properties.

2.1. The quantum dot Hamiltonian

The Hamiltonian used to represent a two-dimensional QD with a single carrier in the presence of an external uniform magnetic field (\mathbf{B}), in addition to an impurity, can be given as:

$$\hat{H} = \frac{(\vec{p} - e\vec{\mathbf{A}})^2}{2m^*} + V_{\text{conf}}(x, y) + V_{\text{imp}}(x, y) + H_{\text{Zeeman}}. \quad (1)$$

The effective mass m^* for the electron depends on the QD material. $\vec{\mathbf{A}}$ is the potential vector that corresponds to the applied \mathbf{B} taken normal to QD plane, in the present work, the symmetric gauge, $\vec{\mathbf{A}} = \frac{B}{2}(-y, x, 0)$, has been used, where the confinement potential is taken to be anisotropic:

$$V_{\text{conf}}(x, y) = \frac{1}{2}m^* (\omega_x^2 x^2 + \omega_y^2 y^2). \quad (2)$$

The confinement potential's shape implies asymmetric electrostatic confinement of the electron in the x and y directions, which may be achieved using appropriate electrostatic gates. By choosing the appropriate values for ω_x and ω_y one can define the shape of the dot from a circle ($\omega_x = \omega_y$) to an ellipse ($\omega_x \neq \omega_y$).

A smooth changing form, finite depth, and range make the Gaussian impurity model an excellent approximation of the impurity potential in QDs. In our current investigation, we picked the impurity potential as:

$$V_{\text{imp}}(x, y) = V_0 e^{-\frac{(x-x_0)^2 + (y-y_0)^2}{d^2}}, \quad (3)$$

where $V_0 > 0$ signifies a repulsive impurity, and (x_0, y_0) specifies the impurity center's position. V_0 measures the impurity potential's strength, whereas d is a measure of the impurity's domain of influence. A large value of d shows that it is spatially distributed, whereas a small value of d accounts for one where the spatial extension of the impurity potential is minimal.

The final term in the Hamiltonian corresponds to the standard Zeeman energy,

$$\hat{H}_{\text{Zeeman}} = \frac{1}{2}g\mu_B\sigma_z. \quad (4)$$

The Schrödinger equation with full Hamiltonian in eq. (1) cannot be solved in an analytic form. As a consequence, the trial wave function has been described in x and y coordinates as a superposition of a product of eigenfunctions of harmonic oscillators,

$$\psi(x, y) = \sum_{n,m} C_{n,m} \phi_n(\alpha_x, x) \phi_m(\alpha_y, y). \quad (5)$$

Here

$$\phi_n(\alpha_x, x) = \frac{1}{\sqrt{2^n n!}} \left(\frac{\alpha_x}{\sqrt{\pi}} \right)^{\frac{1}{2}} e^{-\frac{\alpha_x^2 x^2}{2}} H_n(\alpha_x x), \quad \alpha_x = \left(\frac{m^* \omega_x}{\hbar} \right)^{\frac{1}{2}}; \quad (6)$$

$$\phi_n(\alpha_y, y) = \frac{1}{\sqrt{2^n n!}} \left(\frac{\alpha_y}{\sqrt{\pi}} \right)^{\frac{1}{2}} e^{-\frac{\alpha_y^2 y^2}{2}} H_n(\alpha_y y), \quad \alpha_y = \left(\frac{m^* \omega_y}{\hbar} \right)^{\frac{1}{2}}. \quad (7)$$

By solving the spectral equation $|\langle \Psi_{n_x n_y s} | \hat{H} | \Psi_{n'_x n'_y s'} \rangle - \lambda I| = 0$, the eigenvalues are obtained. Furthermore, eigenvectors are given by the Schrodinger equation with inserted eigenvalues as the energy.

2.2. The magnetic properties of the QD

From the numerical outputs, one can use sufficient energy spectra to calculate the partition function using canonical definition,

$$Z = \sum_n e^{-\beta E_n}, \quad (8)$$

where $\beta = 1/k_B T$, k_B is the Boltzmann constant.

The magnetization (M) of the QD, which indicates the response of the material to \mathbf{B} , is computed as follows [25]:

$$M = -\frac{\partial \langle E \rangle}{\partial B}, \quad (9)$$

where the average energy ($\langle E \rangle$) can be calculated as [10]:

$$\langle E \rangle = -\frac{\partial \text{Ln}(Z)}{\partial \beta}. \quad (10)$$

The magnetic susceptibility (χ) for the system can be computed by taking the derivative of M with respect to B [25] as:

$$\chi = \frac{\partial M}{\partial B}, \quad (11)$$

according to the χ sign, the material can be classified into paramagnetic ($\chi > 0$) and diamagnetic ($\chi < 0$).

3. Results and discussion

This work was done on the InAs anisotropic QD with parameters: $m^* = 0.0239m_0$ and $g = -15$ [26]. The basis-functions with n_x, n_y were taken from 0 – 30 for each direction in the linear variational calculation. The direct product of the basis gave a 30×30 -dimensional space. We confirmed that the basis functions completely cover the two-dimensional space, at least in expressing the observables under investigation. A larger number of basis functions were used in the convergence test. Table 1 shows the eigenenergies for the ground and the first two excited states for a range of basis functions.

TABLE 1. The low-lying states energies for different basis numbers at $V_0 = 32$ meV, $d = 10$ nm, $\omega_x = 4$ meV, $\omega_y = 6$ meV, and $B = 2T$

Space dimension	G. S (meV)	1st excited state (meV)	2nd excited state (meV)
5×5	10.2834	12.9467	20.3453
10×10	10.0443	11.0118	11.3830
15×15	10.0140	10.9043	11.3779
20×20	10.0025	10.8960	11.3750
25×25	9.9996	10.8938	11.3747
30×30	9.9995	10.8938	11.3746
35×35	9.9995	10.8938	11.3746
40×40	9.9995	10.8938	11.3746

In Fig. 1(a,b), we show the Fock-Darwin states of a single electron in the absence of impurity ($V_0 = 0$), for circular QD (Fig. 1(a)) and elliptical QD (Fig. 1(b)). The plots show quite similar behavior of the energies as a function of B , except that the degeneracies of the states are lifted at $B = 0$ due to different confinement strengths in x and y directions; this result has been previously reported in [27]. At $B \neq 0$ the most characteristic feature of the figures is that the Fock-Darwin levels are split due to Zeeman interaction into two substates corresponding to different spin orientations. This separation between the two sublevels shows linear increase with the applied field as $|\mu_B g B|$. Fig. 1(c,d) highlights the effect of on-center gaussian impurity on the state energies of the system as a function of B . An interesting level crossing between the ground state and the first excited state appeared at a particular B . In the isotropic (anisotropic) potential case, this crossing occurs at $B \approx 2.4 T$ ($2.8 T$).

We have studied the dependence of low-lying states on the impurity profiles (strength, influence domain, and position). Fig. 2(a,b,c) shows the effect of the impurity domain on the level crossing; as d increases, the intersection point occurs at a lower magnetic field value. Also, by comparing Figs. 1(d) and 2(a,d), it is revealed that increasing the impurity strength for a fixed influence domain moves the crossing to a lower B value.

In Fig. 3, we plot the low-lying states as a function of impurity strength (Fig. 3(a)) and impurity domain (Fig. 3(b)). The on-center impurity affects the ground state ($|0, 0\rangle$) more than other states, and this increase in the ground state energy makes the levels cross. As V_0 increases, the repulsive force between the impurity and the electron increases; as a result, the electron is pushed from the center to be at a higher energy point. In the same way, as d increases, the impurity effect is spread from the center, so the electron is being pushed further away. Another observation is that when d increases, the excited states are also significantly affected by the impurity potential.

To explain this observation, the electron probability density has been plotted in Fig. 4 for different impurity profiles. As the top panel shows, in the absence of impurity, the electron in state $|0, 0\rangle$ has a higher probability of being at the center of the QD. Since, $\omega_x < \omega_y$ the first excited state ($|1, 0\rangle$) has a node in the x -direction, while the state $|0, 1\rangle$ is the second excited state (which has a node in the y -direction). In the presence of an on-center impurity, the charge density distributes away due to electron-impurity repulsion, so the electron has a greater probability of being further from the center, while for the excited states $|1, 0\rangle$ and $|0, 1\rangle$ the electron probability at the center is zero, so the presence of the impurity has an insignificant effect on the probability, therefore a minor effect on the state's energy, especially for low values of d .

As the impurity strength or its stretch increases, the probability becomes less at the center, so the electron is obligated to be at a higher confined point due to the parabolic well in x and y directions. On the other hand, for a larger value of d (bottom panel of Fig. 4), the effects of impurity on the excited states are apparent, and the effects on the state $|1, 0\rangle$ and $|0, 1\rangle$ varies due to the isotropy of the QD.

From Fig. 5(a), it is clear that the $E_{G.S}$ increases as the impurity strength increases, and the cusp, which corresponds to the crossing, shifts to the left as the strength increases. In Fig. 5(b), the effect of the impurity domain on the $E_{G.S}$ has been displayed. As d increases, more cusps appear in the $E_{G.S}$. For example, two cusps for $d = 20$ nm correspond to the two crossings in Fig. 2(c).

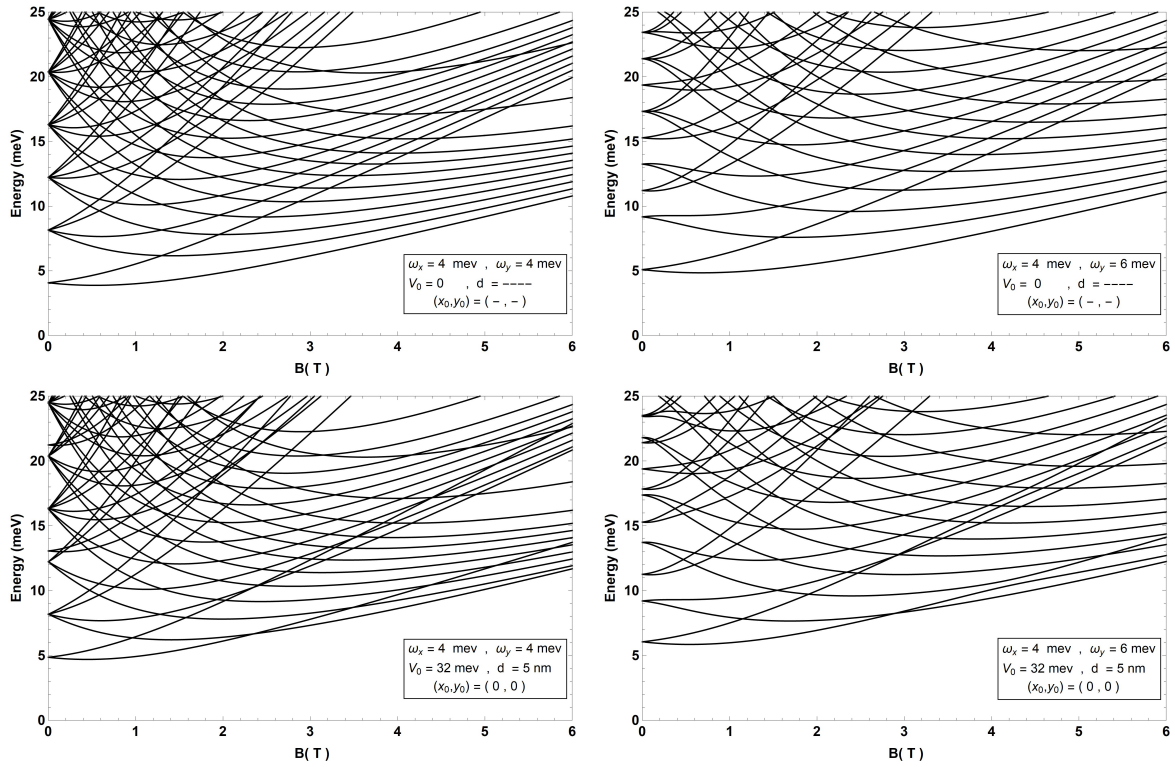


FIG. 1. Low-lying states energies of the QD as a function of B for isotropic (a and c) and anisotropic (b and d)

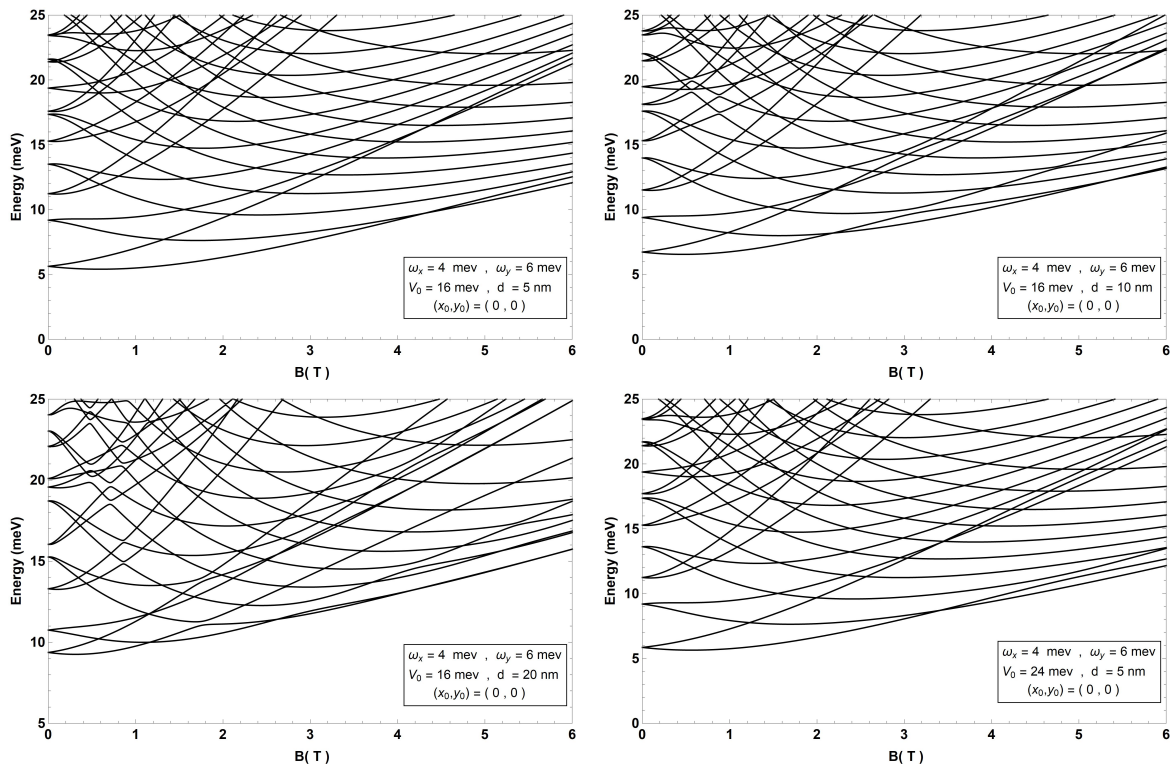


FIG. 2. Low-lying states energies as a function of B for different impurity

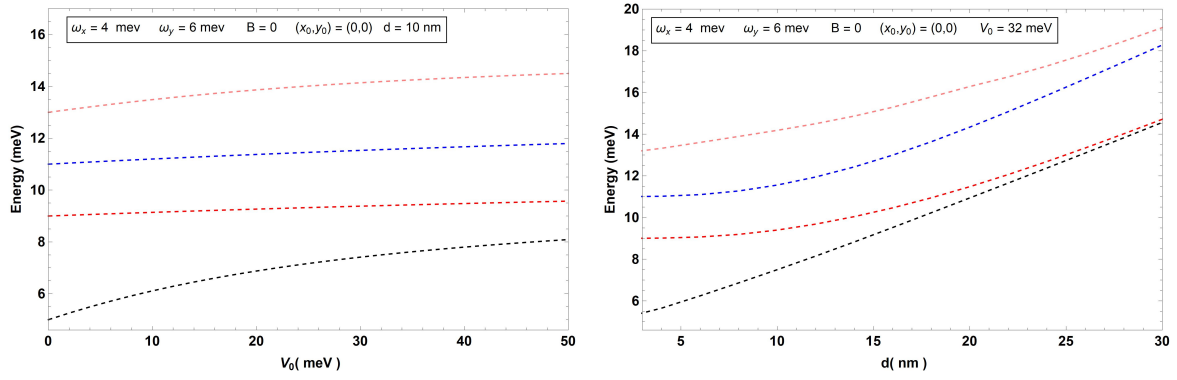


FIG. 3. Low-lying states energies as a function of a) V_0 , b) d for anisotropic potential

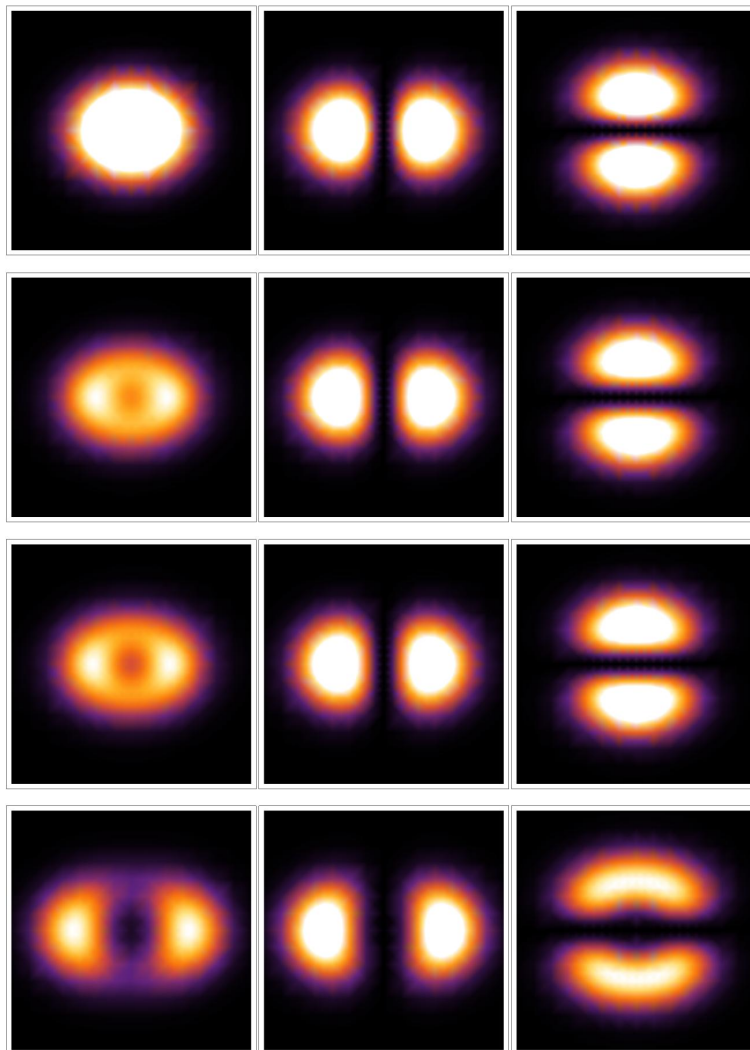


FIG. 4. Probability density $|\psi|^2$ for the wavefunctions of the low-lying states $|0, 0\rangle$, $|1, 0\rangle$, and $|0, 1\rangle$, in the presence of on-center impurity with profiles (from up to down) (V_0, d) : $(0, -)$, $(24, 10)$, $(32, 10)$ and $(32, 20)$ in meV and nm, respectively

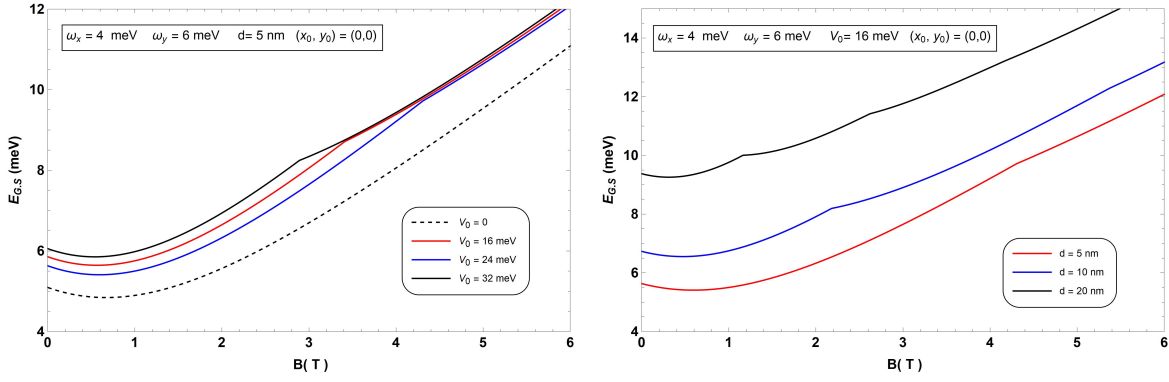


FIG. 5. $E_{G,S}$ as a function of B for different impurity profiles

In Fig. 6, we have displayed the effect of impurity position on the energy level for the four low-lying states. From these two plots, we can conclude that the off-center impurity position affects the states with a larger probability of the electron being at the impurity position; when the impurity is located at $x(y) = 22$ nm from the origin, the energy of the state $|1, 0\rangle$ ($|0, 1\rangle$) is significantly affected, while the states $|0, 1\rangle$ ($|1, 0\rangle$) are minorly affected due to their node at $x(y) = 0$, whereas the third excited state $|2, 0\rangle$ is more affected by the on-center impurity than the lower excited states due to its electron probability at $x = 0$.

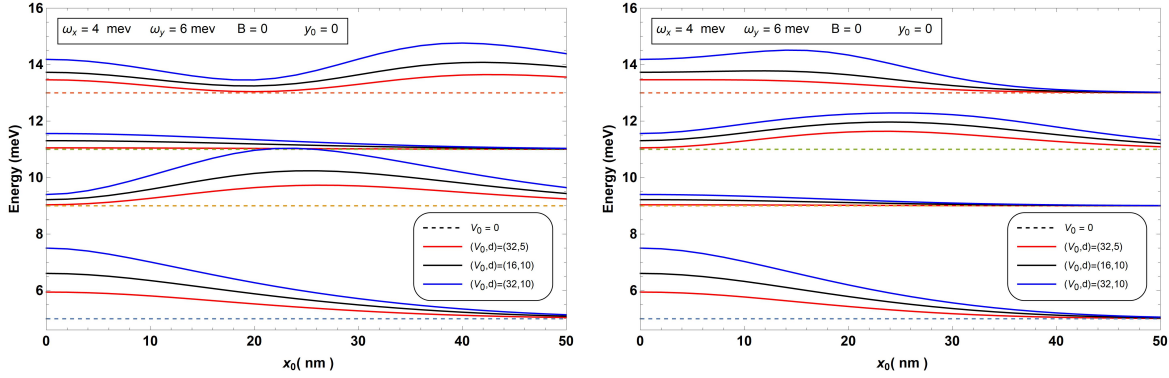


FIG. 6. Impurity position effect on the low-lying energy state

The electron's probability density was calculated and plotted in Fig. 7 for the previous four orbits to support the result of Fig. 6 and make it more understandable. The density extends perpendicular to the axis, which contains the impurity. As a consequence, the energy value increases.

The average statistical energy has been plotted in Fig. 8 in the presence of on-center impurity for different temperatures, and the figure shows that $\langle E \rangle$ is very similar to the ground state energy at low temperatures $T \rightarrow 0$, $E_{G,S}$ has cusps at the level crossings, where the states are degenerate.

The dependence of the magnetization on the magnetic field and the impurity profile was studied in Fig. 9. The results show the presence of oscillation in the magnetization curve due to the intersection of the low-lying states energies. In Fig. 9(a), the effect of the impurity strength is shown; the increase in the impurity strength pulls the intersection in the energy levels shown in previous figures towards a lower value of the magnetic field.

The influence of impurity expansion has been investigated in Fig. 9(b). It is noticed that there are numerous peaks in the magnetization curve at larger values of d due to the occurrence of multiple changes in the ground state energy, which can be observed by referring to Fig. 5(b).

The influence of the impurity position was investigated in Fig. 9(c) since most of the effect on magnetization is attributable to the ground state at temperatures near zero. As a result, the impurity existence away from the center reduces the oscillation peaks height.

In Fig. 9(d), the effect of the temperature has been illustrated. For $T \rightarrow 0$, at the level crossings, the magnetization is discontinuous; consequently, the susceptibility diverges. At finite temperatures, thermal excitations make the magnetization a continuous and smooth function, and the susceptibility then has the spectral line form with a temperature dependence linewidth, as presented in Fig. 10(a). The number and position of the peaks depend on the impurity profile, as shown in Fig. 10(b).

The full width at half maximum of the spectral line of the susceptibility (FWHM) is shown as a function of temperature in Fig. 11. One can see that the temperature changes the spectral linewidth linearly.

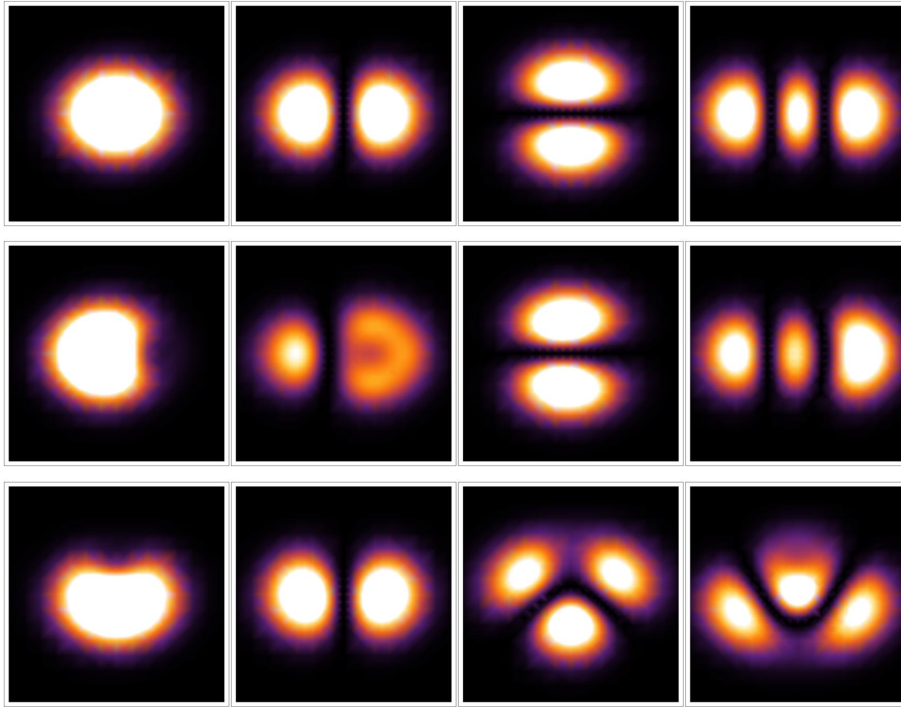


FIG. 7. Probability density $|\psi|^2$ for the wavefunctions of the low-lying states, the top panel for $V_0 = 0$ and the other two panels in the presence of an off-center impurity with $V_0 = 32$ meV and $d = 10$ nm, located at (x_0, y_0) : $(22, 0)$, $(0, 22)$ from up to down respectively

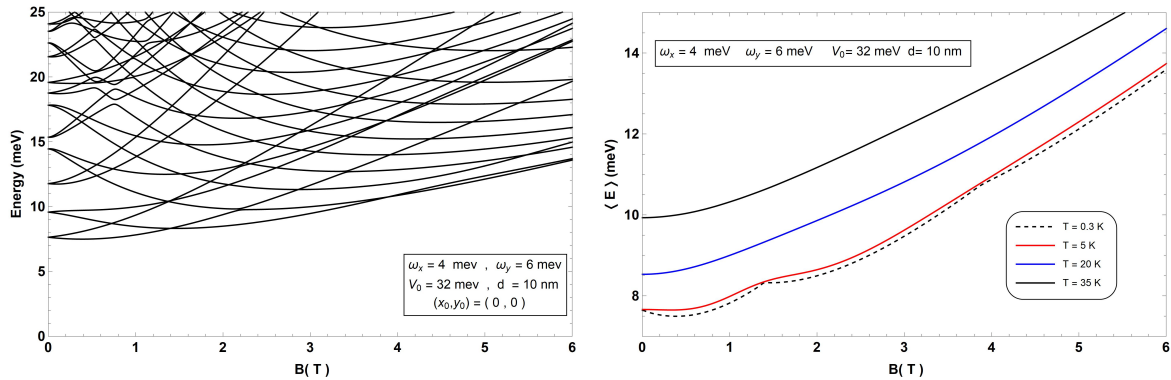


FIG. 8. a) the energy spectra; b) $\langle E \rangle$ vs. the magnetic field for fixed impurity profiles

4. Conclusion

Finally, the Hamiltonian of an electron confined in a 2D anisotropic quantum dot in the presence of acceptor Gaussian impurity has been studied. The obtained numerical energies have been used to investigate the system statistical energies, magnetization, and magnetic susceptibility. This work has concentrated on the low-lying energy levels crossings corresponding to the ground state transitions. These transitions cause cusps in the statistical average energy and oscillations in the magnetization curve. In addition, the magnetic susceptibility of InAs QD has been shown to have a diamagnetic-paramagnetic phase transition due to the impurity presence. This transition is strongly correlated with the impurity profiles (strength, position, and influence domain), magnetic field, and temperature. In applications, the magnetic phase transition (diamagnetic to paramagnetic transition) should be taken into account when estimating the applicability of material to be involved in future technologies as switching devices, magnetic sensors, and magnetic shielding.

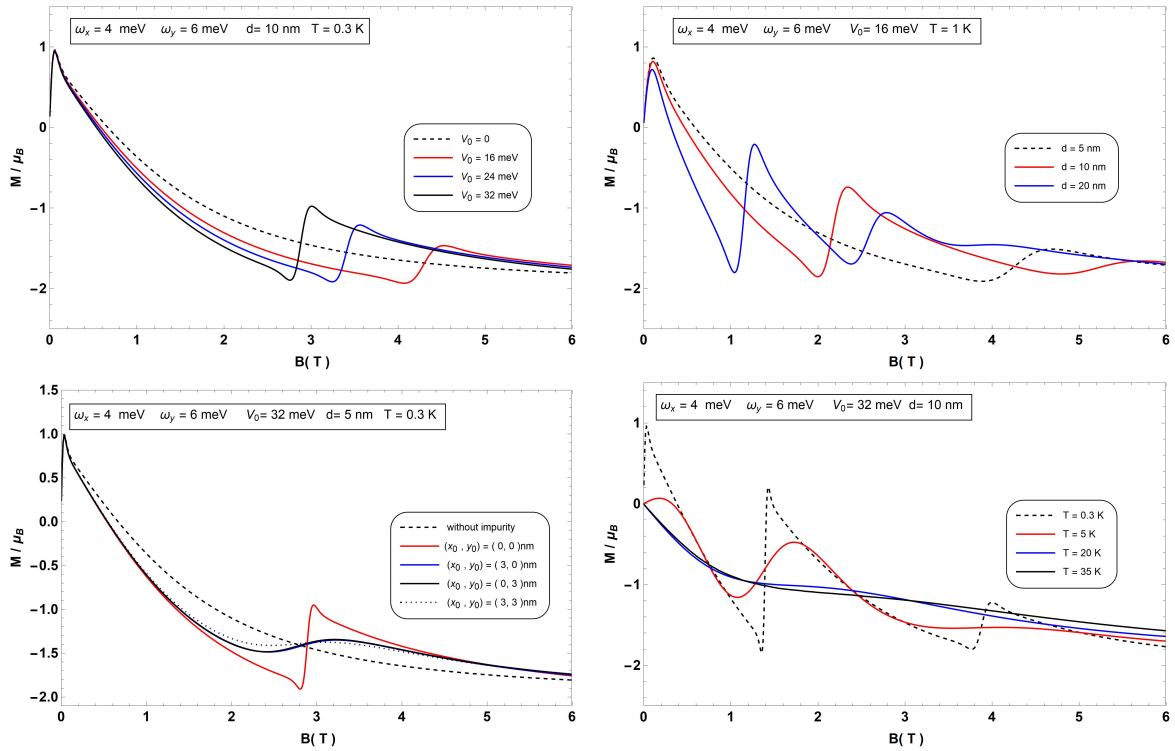


FIG. 9. M vs. B for a) different impurity strengths; b) different impurity stretches; c) different impurity position; and d) different temperature, where all other parameters have been fixed

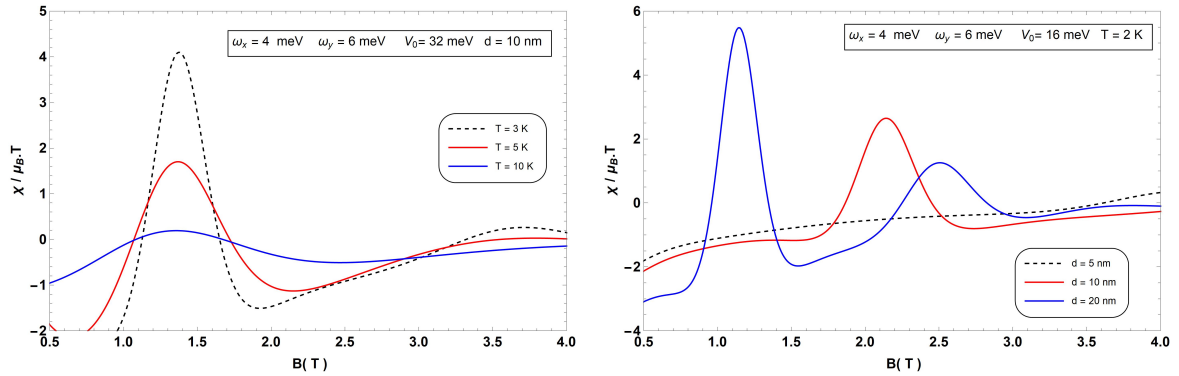


FIG. 10. χ vs. B for a) different temperatures; b) different impurity stretches

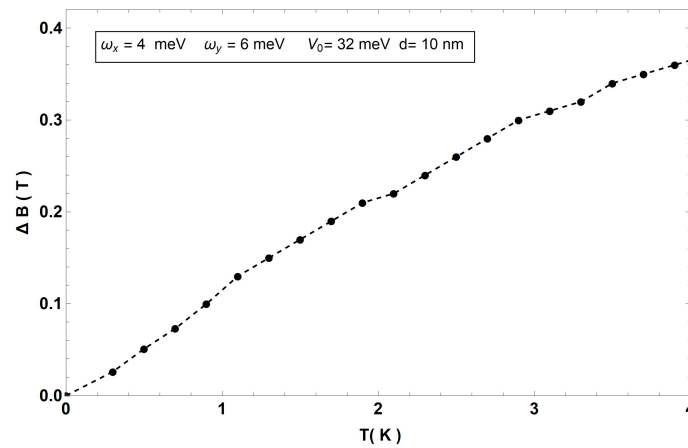


FIG. 11. The full width at half maximum of the spectral linewidth of the susceptibility as a function of temperature

References

- [1] Chakraborty T., Pietiläinen P. Optical signatures of spin-orbit interaction effects in a parabolic quantum dot. *Phys. Rev. Lett.*, 2005, **95** 136603.
- [2] Stufler S., Ester P., Zrenner A., Bichler M. Quantum optical properties of a single $\text{In}_x\text{Ga}_{1-x}\text{As}$ -GaAs quantum dot two-level system. *Phys. Rev. B*, 2005, **72**, 121301.
- [3] Jha P.K., Kumar M., et al. Rashba spin orbit interaction effect on nonlinear optical properties of quantum dot with magnetic field. *Superlattices Microstructures*, 2014, **65**, P. 71–78.
- [4] Gumber S., Kumar M., et al. Thermal and magnetic properties of cylindrical quantum dot with asymmetric confinement. *Canadian J. of Physics*, 2015, **93**, P. 1264–1268.
- [5] Avetisyan S., Chakraborty T., Pietiläinen P. Magnetization of interacting electrons in anisotropic quantum dots with Rashba spin-orbit interaction. *Physica E: Low-dimensional Systems Nanostructures*, 2016, **81**, P. 334–338.
- [6] Gumber S., Kumar M., Jha P.K., Mohan M. Thermodynamic behaviour of Rashba quantum dot in the presence of magnetic field. *Chinese Physics B*, 2016, **25**, 056502.
- [7] Khordad R. The effect of Rashba spin-orbit interaction on electronic and optical properties of a double ring-shaped quantum dot. *Superlattices Microstructures*, 2017, **110**, P. 146–154.
- [8] Baghdasaryan D., Hayrapetyan D., Kazaryan E., Sarkisyan H. Thermal and magnetic properties of electron gas in toroidal quantum dot. *Physica E: Low-dimensional Systems Nanostructures*, 2018, **101**, P. 1–4.
- [9] Castano-Yepes J.D., Amor-Quiroz D., Ramirez-Gutierrez C., Gómez E.A. Impact of a topological defect and Rashba spin-orbit interaction on the thermo-magnetic and optical properties of a 2D semiconductor quantum dot with Gaussian confinement. *Physica E: Low-dimensional Systems Nanostructures*, 2019, **109**, P. 59–66.
- [10] Shaer A., Hjaz E., Elsaid M. The heat capacity of a semiconductor quantum dot in magnetic fields. *Nanosystems: Phys. Chem. Math.*, 2019, **10**, P. 530–535.
- [11] Yahyah N.S., Elsaid M.K., Shaer A. Heat capacity and entropy of Gaussian spherical quantum dot in the presence of donor impurity. *J. of Theor. and Appl. Phys.*, 2019, **13**, P. 277–288.
- [12] Yaseen A., Shaer A., Elsaid M.K. The magnetic properties of GaAs parabolic quantum dot in the presence of donor impurity, magnetic and electric fields. *Chinese J. of Physics*, 2019, **60**, P. 598–611.
- [13] Kandemir B., Cetin A. Impurity magnetopolaron in a parabolic quantum dot: the squeezed-state variational approach. *J. of Phys.: Condensed Matter*, 2005, **17**, 667.
- [14] Datta N.K., Ghosh M. Impurity strength and impurity domain modulated frequency-dependent linear and second nonlinear response properties of doped quantum dots. *Physica Status Solidi*, 2011, **248**, P. 1941–1948.
- [15] Boda A., Chatterjee A. Transition energies and magnetic properties of a neutral donor complex in a Gaussian GaAs quantum dot. *Superlattices Microstructures*, 2016, **97**, P. 268–276.
- [16] Krevchik V.D., Razumov A.V., et al. Temperature dependence of recombination radiation in semiconductor nanostructures with quantum dots containing impurity complexes. *Nanosystems: Phys. Chem. Math.*, 2021, **12**, P. 680–689.
- [17] Shaer A., Elsaid M.K., Elhasan M. Variational calculations of the heat capacity of a semiconductor quantum dot in magnetic fields. *Chinese Journal of Physics*, 2016, **54**, P. 391–397.
- [18] Ciftja O., Faruk M.G. Two-dimensional quantum-dot helium in a magnetic field: Variational theory. *Phys. Rev. B*, 2005, **72**, 205334.
- [19] Alia A.A., Elsaid M.K., Shaer A. Magnetic properties of GaAs parabolic quantum dot in the presence of donor impurity under the influence of external tilted electric and magnetic fields. *J. of Taibah University for Science*, 2019, **13**, P. 687–695.
- [20] Ali M., Elsaid M., Shaer A. Magnetization and magnetic susceptibility of GaAs quantum dot with Gaussian confinement in applied magnetic field. *Jordan J. of Physics*, 2019, **12**, P. 247–254.
- [21] Sharma H.K., Boda A., Boyacioglu B., Chatterjee A. Electronic and magnetic properties of a two-electron Gaussian GaAs quantum dot with spin-Zeeman term: A study by numerical diagonalization. *J. of Magnetism Magnetic Materials*, 2019, **469**, P. 171–177.
- [22] Voskoboynikov O., Bauga O., Lee C., Tretyak O. Magnetic properties of parabolic quantum dots in the presence of the spin-orbit interaction. *J. of Applied Physics*, 2003, **94**, P. 5891–5895.
- [23] Hosseinpour P. The role of Rashba spin-orbit interaction and external fields in the thermal properties of a doped quantum dot with Gaussian impurity. *Physica B: Condensed Matter*, 2020, **593**, 412259.
- [24] Madhav A., Chakraborty T. Electronic properties of anisotropic quantum dots in a magnetic field. *Phys. Rev. B*, 1994, **49**, 8163.
- [25] Shaer A., Elsaid M., Elhasan M. The magnetic properties of a quantum dot in a magnetic field. *Turkish J. of Physics*, 2016, **40**, P. 209–218.
- [26] Prabhakar S., Reynolds J.E., Melnik R. Manipulation of the Landé g factor in InAs quantum dots through the application of anisotropic gate potentials: Exact diagonalization, numerical, and perturbation methods. *Phys. Rev. B*, 2011, **84**, 155208.
- [27] Avetisyan S., Pietiläinen P., Chakraborty T. Strong enhancement of Rashba spin-orbit coupling with increasing anisotropy in the Fock-Darwin states of a quantum dot. *Phys. Rev. B*, 2012, **85**, 153301.

Submitted 30 April 2022; revised 7 May 2022; accepted 8 May 2022

Information about the authors:

Ayham Shaer – Physics Department, An- Najah National University, Nablus, Palestine; ORCID 0000-0002-6518-6470; ayham.shaer@najah.edu

Mohammad K. Elsaid – Physics Department, An- Najah National University, Nablus, Palestine; ORCID 0000-0002-1392-3192; mkelsaid@najah.edu

Conflict of interest: the authors declare no conflict of interest.